

PAPER

Optimization and growth in first-passage resetting

To cite this article: B De Bruyne *et al* *J. Stat. Mech.* (2021) 013203

View the [article online](#) for updates and enhancements.



IOP | **ebooks**TM

Bringing together innovative digital publishing with leading authors from the global scientific community.

Start exploring the collection—download the first chapter of every title for free.

PAPER: Classical statistical mechanics, equilibrium and non-equilibrium

Optimization and growth in first-passage resetting

B De Bruyne^{1,2}, J Randon-Furling^{3,4,5} and S Redner^{6,*}

¹ Perimeter Institute, 31 Caroline Street North, Waterloo, ON, N2L 2Y5, Canada

² LPTMS, CNRS, Univ. Paris-Sud, Université Paris-Saclay, 91405 Orsay, France

³ SAMM, Université Paris 1–FP2M (FR2036) CNRS, 75013 Paris, France

⁴ Department of Mathematics, Columbia University, New York, NY 10027, United States of America

⁵ MSDA, Mohammed VI Polytechnic University, Ben Guerir 43150, Morocco

⁶ Santa Fe Institute, 1399 Hyde Park Rd., Santa Fe, NM 87501, United States of America

E-mail: redner@santafe.edu

Received 9 September 2020

Accepted for publication 29 October 2020

Published 5 January 2021



Online at stacks.iop.org/JSTAT/2021/013203

<https://doi.org/10.1088/1742-5468/abcd33>

Abstract. We combine the processes of resetting and first passage, resulting in *first-passage resetting*, where the resetting of a random walk to a fixed position is triggered by the first-passage event of the walk itself. In an infinite domain, first-passage resetting of isotropic diffusion is non-stationary, and the number of resetting events grows with time according to \sqrt{t} . We analytically calculate the resulting spatial probability distribution of the particle, and also obtain the distribution by geometric-path decomposition. In a finite interval, we define an optimization problem that is controlled by first-passage resetting; this scenario is motivated by reliability theory. The goal is to operate a system close to its maximum capacity without experiencing too many breakdowns. However, when a breakdown occurs the system is reset to its minimal operating point. We define and optimize an objective function that maximizes reward for being close to the maximum level of operation and imposes a penalty for each breakdown. We also investigate extensions of this basic model, firstly to include a delay after each reset, and also to two dimensions. Finally, we study the growth dynamics of a

*Author to whom any correspondence should be addressed.

Optimization and growth in first-passage resetting

domain in which the domain boundary recedes by a specified amount whenever the diffusing particle reaches the boundary, after which a resetting event occurs. We determine the growth rate of the domain for a semi-infinite line and a finite interval and find a wide range of behaviors that depend on how much recession occurs when the particle hits the boundary.

Keywords: diffusion, stochastic processes, fluctuation phenomena

Contents

1. Introduction	3
2. First-passage resetting in semi-infinite geometry	4
2.1. The reset probability distribution	5
2.2. Spatial-probability distribution	5
2.3. Average number of resets	7
2.4. Biased diffusion	8
3. Optimization in first-passage resetting	9
3.1. The finite interval	10
3.2. Time delay for repair	13
3.3. Two dimensions	15
4. Domain growth by first-passage resetting	17
4.1. Expanding semi-infinite geometry	17
4.1.1. Additive growth: $L_n = L_{n-1} + L$	18
4.1.2. Multiplicative growth: $L_n = \alpha L_{n-1}, \alpha > 1$	18
4.2. Expanding interval	19
5. Summary and discussion	22
Acknowledgments	24
Appendix A. Laplace transform approach in semi-infinite geometry	24
A.1. Spatial probability distributions	24
A.2. Average number of resets	26
Appendix B. Solution to the convection-diffusion equation	27
Appendix C. First-passage resetting in the annular geometry	27
Appendix D. Expanding semi-infinite geometry: Laplace transforms	29
D.1. Additive growth: $L_n = L_{n-1} + L$	29
D.2. Multiplicative growth: $L_n = \alpha L_{n-1}, \alpha > 1$	30
Appendix E. Expanding interval: saddle point approximation	31
References	31

1. Introduction

Random walks are ubiquitous in phenomena across a wide range of fields, such as physics, chemistry, finance and social sciences [1–4]. In addition to the applications of the random walk, many useful extensions of the basic model have been developed (see, e.g. [5–8]). Almost a decade ago, the notion of resetting a random walk was introduced [9–11]. The basic idea of resetting is simplicity itself: at a given rate, a random walk is reset to its starting point. The rich phenomenology induced by this extension of the random walk has sparked much interest (see, e.g. [9–19]). In the context of search strategies, where the walker is searching for a target at a fixed location, resetting changes the average search time from infinite (when the domain is infinite) to finite [20–23]. Moreover, an optimal resetting rate exists, which minimizes the search time. A very different, but also fruitful concept in the theory of random walks is the notion of a first-passage process [2, 24–26]. Of particular importance is first-passage probability, which is defined as the probability that a walker reaches a specified location for the first time. This notion has many applications in situations where a particular event happens when a threshold is first reached. One such example is a limit order for a stock. When the price of a stock, whose evolution is often modeled as a geometric random walk, first reaches a limit price, this event triggers the sale or the purchase of the stock.

In this work, we combine these disparate notions of first passage and resetting into *first-passage resetting*, in which a particle is reset whenever it reaches a specified threshold. Contrary to standard resetting, the time at which first-passage resetting occurs is defined by the motion of the diffusing particle itself, rather than being imposed externally [9–11]. Feller showed that such a process is well defined mathematically and provided existence and uniqueness theorems [27], while similar ideas were pursued in [28]. First-passage resetting was initially treated in the physics literature for the situation in which two Brownian particles are biased toward each other, and they are reset to their initial positions when they encounter each other [29].

In our work, we first focus on the related situation of a diffusing particle on a semi-infinite line $x \leq L$ that is reset to the origin whenever the particle hits a boundary $x = L$ (figure 1). The model studied in [29] corresponds to a drift toward the boundary in our semi-infinite geometry; this setting leads to a stationary state. In contrast, the absence of drift in our model leads to a variety of new phenomena. In particular, the probability distribution for the position of the particle is non-stationary. We also construct two simple path decompositions for first-passage resetting, in which the trajectory of the resetting particle is mapped onto a free-diffusion process. This approach provides useful geometrical insights, as well as simple ways to derive the average number of reset events and the spatial probability distribution with essentially no calculation.

We then treat first-passage resetting at a finite interval, which has a natural application to reliability theory. Here, the particle is restricted to the interval $[0, L]$ where $x = L$ is again the boundary where resetting occurs, and the particle is immediately reinjected at $x = 0$ when it reaches $x = L$. We may view this mechanism as

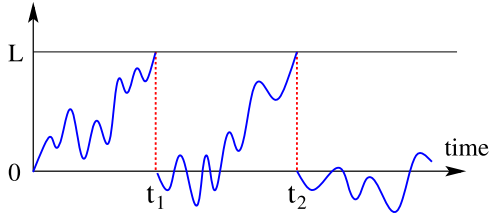


Figure 1. Schematic illustration of first-passage resetting for diffusion on a semi-infinite line $x \leq L$. Each time the particle reaches the threshold L , it is reset to the origin. The times of the resetting events are denoted by t_1, t_2, \dots .

characterizing the performance of a driven mechanical system [30–33], with the coordinates $x = 0$ and $x = L$ indicating poor and maximal performances, respectively. While one ideally wants to operate the system close to its maximum performance level ($x = L$), there is a risk of overuse, leading to breakdowns whenever $x = L$ is reached. Subsequently, the system has to be repaired and then restarted from $x = 0$. This dynamic corresponds to resetting that is induced by a first passage to the boundary $x = L$. We will find the optimal bias velocity that optimizes the performance of the system. We will also investigate additional features of this first-passage resetting, such as a random maintenance delay at each breakdown and resetting in higher dimensions. A preliminary account of some of these results was given in [34].

Finally, we investigate a very different aspect of first-passage resetting, where the domain boundary at which resetting occurs moves by a specified amount each time the diffusing particle reaches this boundary. Many features of this moving-boundary problem can be readily calculated because of the renewal structure of the theory. For both the semi-infinite and finite-interval geometries, we find a variety of scaling behaviors for the motion of the resetting boundary. These behaviors depend on the initial geometry and by how much the boundary moves at each resetting event.

2. First-passage resetting in semi-infinite geometry

In the standard resetting process, reset events occur at a fixed rate r and are uncorrelated with the position of the diffusing particle. In contrast, first-passage resetting directly couples the times at which resetting occurs and the particle position. For first-passage resetting in a semi-infinite line geometry, the particle starts at $x(0) = 0$ and freely diffuses in the range $x \leq L$ (with $L > 0$). Each time L is reached, the particle is instantaneously reset to the origin (figure 1). We are interested in two basic characteristics of the particle's motion: the spatial probability distribution of the particle and the time dependence of the number of reset events. To compute these quantities, we rely on the renewal structure of the process, which allows us to first compute the probability for n reset events in a direct way. With this result, as well as the propagator for free diffusion in the presence of an absorbing boundary, we can readily obtain the spatial distribution of the particle and the average number of resets in a given time.

2.1. The n th reset probability distribution

We define $F_n(L, t)$ as the probability that the particle resets for the n th time at time t . When $n = 1$, this quantity is the standard first-passage probability for a freely diffusing particle that starts at the origin, to first reach L [25, 26]:

$$F_1(L, t) \equiv F(L, t) = \frac{L}{\sqrt{4\pi D t^3}} e^{-L^2/4Dt}.$$

For the particle to reset for the n th time at a time t with $n > 1$, the particle must reset for the $(n - 1)$ th time at some earlier time $t' < t$, and reset again at time t . Because the process is renewed at each reset, $F_n(L, t)$ is formally given by the renewal equation

$$F_n(L, t) = \int_0^t dt' F_{n-1}(L, t') F_1(L, t - t'), \quad n > 1. \quad (1a)$$

The convolution structure of equation (1a) lends itself to a Laplace transform analysis. The corresponding equation in the Laplace domain is simply:

$$\tilde{F}_n(L, s) = \tilde{F}_{n-1}(L, s) \tilde{F}_1(L, s) = \tilde{F}_1(L, s)^n, \quad (1b)$$

where quantities with tildes denote Laplace transforms. Using the Laplace transform of the first-passage probability:

$$\tilde{F}_1(L, s) = \int_0^\infty dt F_1(L, t) e^{-s t} = e^{\sqrt{sL^2/D}} \equiv e^{-\ell},$$

where we define the scaled coordinate $\ell \equiv \sqrt{s/D} L$ henceforth, then equation (1b) becomes

$$\tilde{F}_n(L, s) = e^{-n\ell}.$$

Notice that $\tilde{F}_n(L, s)$ has the same form as $\tilde{F}_1(L, s)$ with $L \rightarrow nL$. That is, the time required for a diffusing particle to reset n times at a fixed boundary $x = L$ is the same as the time taken for a freely diffusing particle to first reach $x = nL$.

In hindsight, this equivalence between the first-passage probability of reaching $x = nL$ and the n th-passage probability of reaching $x = L$ with resetting at $x = L$ is self-evident. As indicated in figure 2 for the case $n = 3$, a first-passage path from zero to $3L$ is composed of a first-passage path from zero to L , followed by a first-passage path from L to $2L$, and finally a first-passage path from $2L$ to $3L$. Resetting causes each of these three segments to (re)start from the origin. Thus, the point $x = L$ is first reached for the third time after resetting has taken place by these displaced paths.

2.2. Spatial-probability distribution

We now compute the probability distribution of the diffusing particle at time t , $P(x, t)$, on the semi-infinite line $x \leq L$ under the influence of first-passage resetting. This distribution can be obtained in several ways. Here, we make use of the path transformation

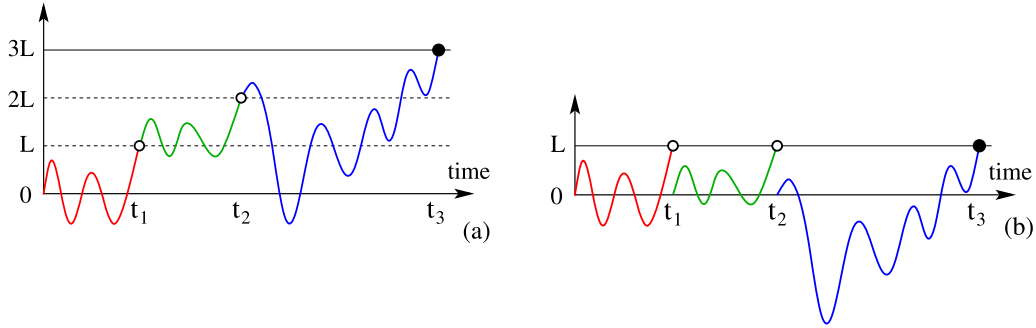


Figure 2. Relation between a first-passage path to $x = 3L$ and a third-passage path to $x = L$, with resetting each time $x = L$ is reached. The green and blue paths in (b) have merely been shifted vertically downward by L and $2L$ compared to (a), respectively.

discussed above for the derivation of the n th passage probability (see figure 2). (A calculational approach based on Laplace transforms that relies on the renewal structure of the process is given in appendix A.) When the walker is at position $x \in [0, L]$ at time t and has experienced exactly n resets, this is equivalent to a free particle being at a position $x + nL$ without having reached level $(n + 1)L$. As a result, the corresponding probability is that of a free particle with a position $x(t) = x + nL$ and a running maximum position $M(t) < (n + 1)L$; the latter is defined by $M(t) = \max_{t' \leq t} x(t')$. The joint distribution of the position and the maximum, $x(t) = x$ and $M(t) = m$, is given by

$$\Pi(x, m, t) = \frac{2m - x}{\sqrt{4\pi D^3 t^3}} e^{-(2m-x)^2/4Dt}. \quad (2)$$

This formula was established by Lévy [35, 36] and it can be derived using the reflection property of Brownian motion. From this joint probability, we find that

$$\begin{aligned} P(x, t) &= \sum_{n \geq 0} \text{Prob}(M(t) < (n + 1)L \text{ and } x(t) = x + nL) \\ &= \sum_{n \geq 0} \int_{x+nL}^{(n+1)L} dm \Pi(x + nL, m, t) \\ &= \frac{1}{\sqrt{4\pi D t}} \sum_{n \geq 0} \left[e^{-(x+nL)^2/4Dt} - e^{-[x-(n+2)L]^2/4Dt} \right], \quad 0 < x \leq L. \end{aligned} \quad (3)$$

While this expression is exact, it is not in a convenient form for its long-term behavior to be determined. However, the long-term limit of $P(x, t)$ can be simply obtained by expanding its Laplace transform (see [34]) for small s ,

$$\tilde{P}(x, s) \simeq \frac{1}{\sqrt{Ds}} \frac{L - x}{L} \quad 0 \leq x \leq L, \quad s \rightarrow 0, \quad (4a)$$

from which the inverse Laplace transform is

$$P(x, t) \simeq \frac{1}{\sqrt{\pi D t}} \frac{L-x}{L} \quad 0 \leq x \leq L, \quad t \rightarrow \infty. \quad (4b)$$

The linear x dependence arises from the balance between the diffusive flux that exits at the reset point $x = L$ and this same flux being re-injected at $x = 0$.

For $x < 0$, the integral in the second line of (3) ranges from nL to $(n+1)L$ rather than from $x + nL$. This leads to

$$\begin{aligned} P(x, t) &= \frac{1}{\sqrt{4\pi D t}} \sum_{n \geq 0} \left[e^{-(x-nL)^2/4Dt} - e^{-(x-(n+2)L)^2/4Dt} \right] \\ &= \frac{1}{\sqrt{4\pi D t}} \left[e^{-x^2/4Dt} + e^{-(x-L)^2/4Dt} \right], \quad x < 0. \end{aligned} \quad (5)$$

Thus, the probability distribution is merely the sum of two Gaussians. In the long-term limit and for $|x|/\sqrt{4Dt} \gg 1$, the factor L in the second term becomes irrelevant and the distribution reduces to that of diffusion on the half line in the presence of a reflecting boundary.

An appealing way to obtain the probability distribution (5) is by a path decomposition construction. Consider the original resetting problem and partition all trajectories into those that undergo either an odd or an even number of resets. In the former case, we invert the segments *before* each odd-numbered resetting about the origin and then translate each such segment by a distance $+L$ (blue arrows in figures 3(a) and (c)). As shown in this portion of the figure, the resulting trajectory is simply a Brownian path that starts at $x = L$ and propagates freely to its final position x . For a path that consists of an even number of resetting events, we perform this same inversion and translation on the segments *after* each odd-numbered resetting (green arrows in figures 3(b) and (d)). The resulting trajectory is now a Brownian path that starts at the origin and propagates freely to its final position x . It is worth emphasizing that this decomposition applies for any symmetric and continuous stochastic process (provided it is homogeneous and stationary).

2.3. Average number of resets

To find the average number of resets that occur up to time t , we first compute the probability that n resets have occurred during this time. By relying on the path transformation shown in figure 2, we find that the probability for exactly n resets to have occurred by time t equals the probability for a freely diffusing particle to have a running maximum $M(t)$ greater than nL but less than $(n+1)L$, that is:

$$P(N(t) = n) = \text{Prob}(nL \leq M(t) < (n+1)L). \quad (6)$$

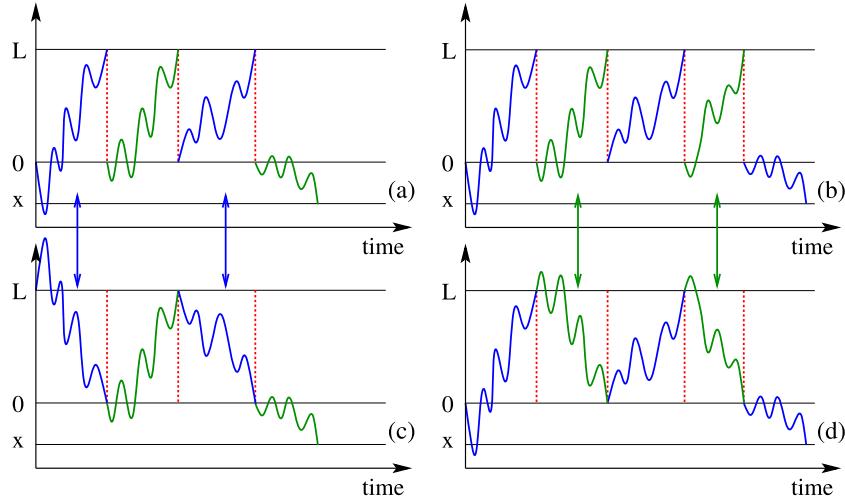


Figure 3. Schematic space-time trajectory of diffusion with first-passage resetting on a semi-infinite line. (a) A path with an odd number of resets is equivalent to (c) a freely diffusing path that starts at $x(t=0) = L$. (b) A path with an even number of resets is equivalent to (d) a freely diffusing path that starts from $x(t=0) = 0$. This equivalence underlies the spatial probability distribution for $x < 0$ in equation (5).

The distribution of $M(t)$ is known [36–38] and may be readily rederived from (2),

$$P(M(t) = m) = \frac{1}{\sqrt{\pi D t}} e^{-m^2/4Dt},$$

from which it follows that

$$P(N(t) = n) = \operatorname{erf}\left(\frac{(n+1)L}{\sqrt{4Dt}}\right) - \operatorname{erf}\left(\frac{nL}{\sqrt{4Dt}}\right), \quad (7)$$

where erf is the Gauss error function.

We can compute the average number of reset events, $\mathcal{N}(t) \equiv \langle N(t) \rangle$, from (7), but it is quicker to reuse the mapping with the running maximum of free diffusion. Indeed, writing $\mathcal{M}(t)$ for the average maximum position of a freely diffusing particle up to time t , one has

$$\mathcal{N}(t)L \leq \mathcal{M}(t) < [\mathcal{N}(t) + 1]L. \quad (8)$$

Since $\mathcal{M}(t) = \sqrt{4Dt/\pi}$, we find that the long-term behavior of $\mathcal{N}(t)$ is given by

$$\mathcal{N}(t) \simeq \sqrt{4Dt/\pi L^2}. \quad (9)$$

The resetting process is non-stationary, as the number of reset events grows according to \sqrt{t} .

2.4. Biased diffusion

The case where the diffusing particle is biased toward the resetting boundary is equivalent to the model studied by Falcao and Evans [29]. Here we briefly discuss the complementary situation in which the particle is biased away from the resetting boundary, with a drift velocity $v < 0$. In the absence of resetting, a particle that starts at the origin eventually reaches $x = L$ with a probability $H = e^{-Pe}$, and escapes to $x = -\infty$ with a probability $1 - H$ [24, 25], where $Pe \equiv vL/2D$ is the Péclet number (the dimensionless bias velocity). When resetting can occur, H now becomes the probability that a resetting event actually happens. Consequently, the probability that the particle resets exactly n times is given by $R_n = H^n(1 - H)$. The average number of resetting events before ultimate escape is therefore

$$\mathcal{N}(t) = \sum_n n R_n = \frac{H}{1 - H} = \frac{1}{e^{Pe} - 1}. \quad (10)$$

In the limit of $v \rightarrow 0$, the number of resetting events diverges as $\mathcal{N}(t) \simeq 2D/(vL)$. The time between resetting events is known to be L/v [25, 39]. Thus after typically $1/(e^{Pe} - 1)$ resetting events, each of which requires a time of L/v , the particle escapes to $-\infty$.

We can also compute the spatial probability distribution of the particle when it undergoes biased diffusion with a bias velocity of magnitude v . Again, we make use of the path transformation shown in figure 2. For a Brownian particle with drift v , the analog of equation (2) is [35]

$$\Pi(x, m, t) = \frac{2m - x}{\sqrt{4\pi D^3 t^3}} e^{-(2m-x)^2/4Dt} e^{Pe(x/L - Pe Dt/L^2)}, \quad (11)$$

which leads to

$$P(x, t) = \frac{1}{\sqrt{4\pi D t}} \sum_{n \geq 0} \left[e^{-(x+nL)^2/4Dt} - e^{-(x-(n+2)L)^2/4Dt} \right] e^{Pe(x/L + n - Pe Dt/L^2)}, \quad 0 < x \leq L \quad (12a)$$

and

$$P(x, t) = \frac{1}{\sqrt{4\pi D t}} \sum_{n \geq 0} \left[e^{-(x-nL)^2/4Dt} - e^{-(x-(n+2)L)^2/4Dt} \right] e^{Pe(x/L + n - Pe Dt/L^2)}, \quad x < 0. \quad (12b)$$

In contrast to the driftless case, there is no simplification for the probability distribution when $x < 0$. In particular, the path transformation of figure 3 requires symmetry and thus does not hold in the presence of drift.

3. Optimization in first-passage resetting

3.1. The finite interval

We now introduce an optimization problem that arises due to first-passage resetting. We envisage a mechanical system whose operating coordinate $x(t)$ lies in the range $[0, L]$. Increasing the value of x corresponds to increasing its operational performance, and it is desirable to run the system as close as possible to its maximum capacity, L . However, the system breaks down whenever x reaches L , after which repairs have to be made before the system can then restart its operation from $x = 0$. While the dynamics of the operating coordinate are typically complicated and dependent on multiple parameters, we view the coordinate x as undergoing a drift-diffusion process for the sake of parsimonious modeling. For the system to be close to $x = L$, the drift should be positive. On the other hand, breakdowns of the system are to be avoided because a cost is incurred by each breakdown. This suggests that the drift velocity should be negative. The goal is to determine the optimal operation that maximizes the performance of the system as a function of the cost for each breakdown and the drift velocity. Although the analogy between first-passage resetting and a mechanical system is naive, this formulation allows us to determine the optimal operation in a concrete way.

The basic control parameter is the magnitude of the drift velocity. If the velocity is large and negative, the system is under-exploited because it operates far from its maximum capacity. Conversely, if the velocity is large and positive, the system breaks down often. We seek the optimal operation by maximizing an objective function, \mathcal{F} , that rewards high performance and penalizes breakdowns. A natural choice for \mathcal{F} is

$$\mathcal{F} = \lim_{T \rightarrow \infty} \frac{1}{T} \left[\frac{1}{L} \int_0^T x(t) dt - C \mathcal{N}(T) \right], \quad (13)$$

where T is the total operational time, $\mathcal{N}(T)$ is the average number of breakdowns within a time T , where T is much longer than the mean breakdown time, and C is the cost of each breakdown. As defined, this objective function rewards operation close to the maximum point L and penalizes breakdowns.

We now determine this objective function when the operating coordinate $x(t)$ evolves according to drift-diffusion, with the additional constraint that $x(t)$ is reset to zero whenever x reaches L . Mathematically, we need to solve the convection–diffusion equation with the following additional conditions: (i) a δ -function source at the origin whose magnitude is determined by the outgoing flux $j(x) = -D\partial_x c + vc$ at $x = L$, (ii) a reflecting boundary condition at $x = 0$, and (iii) the initial condition $x(t = 0) = 0$. That is, we want to solve

$$\partial_t c + v\partial_x c = D\partial_{xx} c + \delta(x)(-D\partial_x c + vc)|_{x=L}, \quad (14a)$$

subject to

$$\begin{cases} (D\partial_x c - vc) |_{x=0} = \delta(t) \\ c(L, t) = 0 \\ c(x, 0) = 0 \end{cases}.$$

Here, $c \equiv c(x, t)$ is the probability density for the operating coordinate, the subscripts denote partial differentiation, D is the diffusion coefficient, and v is the drift velocity. Notice that the reflecting boundary condition at $x = 0$ holds *except* at the start of the process, to account for the unit input of flux at $t = 0$. This construction allows one to take the initial condition to be $c(x, t = 0) = 0$, which greatly simplifies all the calculations. Effectively, this flux initial condition corresponds to starting the system with the particle at $x = 0$. As in section 2, we first solve the free theory, where the delta-function term in (14a) is absent, and then use renewal equations to solve the full problem. In the free case, equation (14a) becomes, in the Laplace domain:

$$s\tilde{c}_0 + v\partial_x\tilde{c}_0 = D\partial_{xx}\tilde{c}_0, \quad (14b)$$

and is subject to the boundary conditions

$$\begin{cases} (D\partial_x\tilde{c}_0 - v\tilde{c}_0) |_{x=0} = 1, \\ \tilde{c}_0(L, s) = 0, \end{cases}$$

where the subscript 0 denotes the concentration without flux re-injection. The solution to (14b) is standard and the result is (see appendix B for details):

$$\tilde{c}_0(x, s) = \frac{2e^P \sinh[w(L-x)]}{\mathcal{W}}, \quad (15a)$$

where $P \equiv vx/2D$, $w = \sqrt{v^2 + 4Ds}/2D$ and $\mathcal{W} = 2Dw \cosh(Lw) + v \sinh(Lw)$. In terms of \tilde{c}_0 , the Laplace transform of the first-passage probability to $x = L$ is

$$\tilde{F}_1(L, s) = (-D\partial_x\tilde{c}_0 + v\tilde{c}_0) |_{x=L} = \frac{2Dw e^{Pe}}{\mathcal{W}}, \quad (15b)$$

where again $Pe = vL/2D$ is the Péclet number. With re-injection of the outgoing flux, the concentration obeys the renewal equations. In the Laplace domain and using \tilde{c}_0 above from the free theory, we obtain

$$\tilde{c}(x, s) = \frac{\tilde{c}_0(x, s)}{1 - \tilde{F}_1(L, s)} = \frac{2e^P \sinh[w(L-x)]}{\mathcal{W} - 2Dw e^{Pe}}, \quad (16)$$

into which we substitute the results from equation (15) to obtain the final result.

Contrary to the semi-infinite case, a stationary distribution is attained on the finite interval. To determine this steady state, we use the duality between the limits $s \rightarrow 0$ in

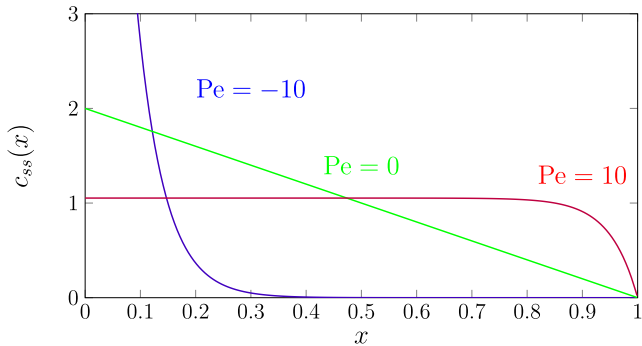


Figure 4. The stationary distribution of the first-passage resetting process in the interval $[0, 1]$ for different Péclet numbers.

the Laplace domain and $t \rightarrow \infty$ in the time domain. With this approach, the coefficient of the term proportional to $1/s$ in $\tilde{c}(x, s)$ gives the steady-state concentration, c_{ss} , in the time domain:

$$c_{ss}(x) \simeq \frac{1}{L} \times \frac{1 - e^{-2(Pe - P)}}{1 - Pe^{-1} e^{-Pe} \sinh(Pe)}, \quad (17)$$

from which the normalized first moment in the steady state is

$$\langle x \rangle = \frac{1}{L} \int_0^L x c(x) dx = \frac{(2Pe^2 - 2Pe + 1) e^{2Pe} - 1}{2Pe [(2Pe - 1) e^{2Pe} + 1]}. \quad (18)$$

Representative plots of the stationary-state concentrations for different Péclet numbers are given in figure 4. As one might anticipate, the density profile is concentrated near $x = 0$ for negative drift velocities, while for positive drift there is a constant cycling of outgoing flux that is reinjected at $x = 0$, which leads to a nearly constant density profile.

The average number of reset events \mathcal{N} satisfies the renewal equation (A.7a), and substituting in \tilde{F}_1 from (15b), we obtain

$$\tilde{\mathcal{N}}(s) = \frac{2D w e^{Pe}}{s [\mathcal{W} - 2Dw e^{Pe}]} \quad (19a)$$

We now extract the long-term behavior for the average number of times that $x = L$ is reached by taking the limit $s \rightarrow 0$ of $\tilde{\mathcal{N}}(s)$ to give

$$\mathcal{N}(T) \simeq \frac{4Pe^2}{2Pe - 1 + e^{-2Pe}} \frac{T}{L^2/D}. \quad (19b)$$

Substituting these expressions for $\langle x \rangle/L$ and \mathcal{N} into (13) immediately gives the objective function, and representative plots are shown in figure 5(a). For a given breakdown cost, there is an optimal drift velocity or an optimal Péclet number. The higher this cost,

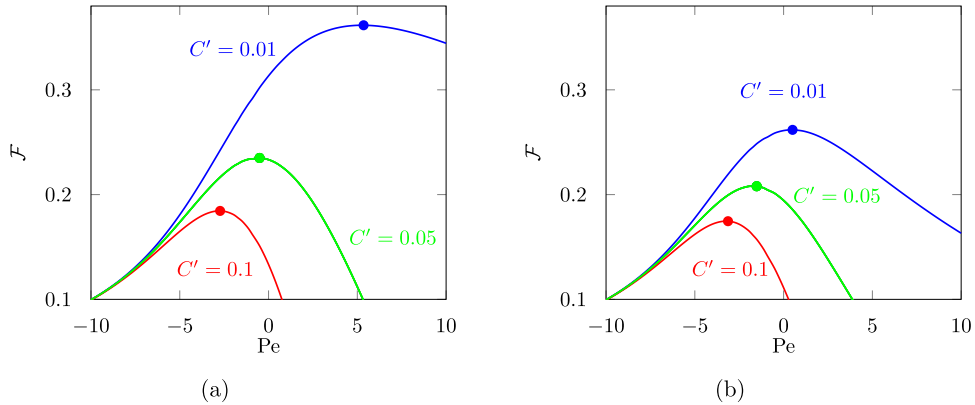


Figure 5. The objective function versus Péclet number Pe for different normalized cost values $C' \equiv C/(L^2/D)$ for: (a) no delay upon resetting, and (b) a dimensionless delay time of $\bar{\tau} = 0.1$ at each resetting. The optimal operating point is indicated on each curve.

the smaller the optimal bias and the value of \mathcal{F} . Moreover, the optimal bias is not necessarily negative. Indeed, if the cost of a breakdown is relatively small, then it is advantageous to operate the system close to its limit, L , and absorb the (small) cost of many breakdowns. On the contrary, if the cost of a breakdown is high, it is better to run the system at a low level and with a negative bias to avoid breakdowns.

3.2. Time delay for repair

When a mechanical system breaks down, there is usually some downtime during which repairs are made before the system can be restarted. This type of downtime can be naturally incorporated into our model by including a random delay time after each resetting event. Thus, when the particle reaches $x = L$ and is returned to $x = 0$, we posit that the particle waits at the origin for a random time τ that is drawn from the exponential distribution $\sigma^{-1} e^{-\tau/\sigma}$ before the particle starts moving again. We now determine the role of this delay on the optimal operation of the system.

The governing renewal equations can be readily extended to incorporate this delay. This delay mechanism can also be viewed as so-called ‘sticky’ Brownian motion [40–42] that is then combined with first-passage resetting. When we include this delay, the renewal equation for the probability distribution becomes:

$$P(x, t) = G(x, L, t) + \int_0^t dt' F_1(t') \left[\delta_0(x) e^{-(t-t')/\sigma} + \int_0^{t-t'} \frac{d\tau}{\sigma} e^{-\tau/\sigma} P(x, t-t'-\tau) \right]. \quad (20a)$$

This equation encapsulates the two possibilities for the subsequent behavior of the particle when it first reaches $x = L$ at time t' . Either the particle remains at $x = 0$ for the remaining time $t - t'$ or the particle waits for a time $\tau < t - t'$ and then the process starts anew from $(x, t) = (0, t' + \tau)$ for the remaining time $t - t' - \tau$. In a similar

fashion, the renewal equation for the average number of resetting events is

$$\mathcal{N}(t) = \int_0^t dt' F_1(t') \left\{ e^{-(t-t')/\sigma} + \int_0^{t-t'} \frac{d\tau}{\sigma} e^{-\tau/\sigma} [1 + \mathcal{N}(t-t'-\tau)] \right\}. \quad (20b)$$

Equation (20b) accounts for the particle first hitting L at a time t' and either waiting at the origin for the entire remaining time $t - t'$ or waiting there for a time $\tau < t - t'$ and then renewing the process for the remaining time. For this latter possibility, there will be, on average, $1 + \mathcal{N}(t - t' - \tau)$ resetting events.

Solving equation (20) in the Laplacian domain yields:

$$\begin{aligned} \tilde{P}(x, s) &= \frac{\delta(x) \sigma \tilde{F}_1(s) + \tilde{G}(x, s)(1 + \sigma s)}{1 - F_1(s) + \sigma s}, \\ \tilde{\mathcal{N}}(s) &= \frac{\tilde{F}_1(s)(\sigma + 1/s)}{1 + s\sigma - \tilde{F}_1(s)}. \end{aligned} \quad (21a)$$

We now use the results from section 3.1 for the optimization problem in the interval with no delay. Namely, we substitute the first-passage probability $\tilde{F}_1(s)$ from equation (15b) into equation (21a) and the probability distribution in equation (15a) for $\tilde{G}(x, s)$ to obtain

$$\begin{aligned} \tilde{P}(x, s) &= \frac{\delta(x) \sigma 2Dw + 2 \sinh(w(L-x))(1 + \sigma s)}{\mathcal{W} e^{-Pe}(1 + \sigma s) - 2Dw}, \\ \tilde{\mathcal{N}}(s) &= \frac{2Dw(\sigma + 1/s)}{\mathcal{W} e^{-Pe}(1 + s\sigma) - 2Dw}. \end{aligned} \quad (21b)$$

From the Laplace transform of the spatial probability density, we compute its stationary distribution by taking the $s \rightarrow 0$ limit and obtain

$$P(x) \simeq \frac{e^{Pe} Pe (2\bar{\tau} Pe L \delta_0(x) + 1) - Pe e^P}{e^{Pe} (\bar{\tau} Pe^2 + Pe - 1) + 1} \frac{1}{L}, \quad (22a)$$

where $\bar{\tau} = D\sigma/L^2$ is the dimensionless delay time. From this distribution, the average position of the particle is

$$\frac{\langle x \rangle}{L} = \frac{[(Pe - 2)Pe + 2] e^{Pe} - 2}{2 [Pe(\bar{\tau} Pe^2 + Pe - 1)e^{Pe} + Pe]}. \quad (22b)$$

Similarly, the average number of resetting events, or equivalently, the average number of breakdowns in the long-term limit is

$$\mathcal{N} = \frac{Pe^2}{Pe - 1 + \bar{\tau} Pe^2 + e^{-Pe}} \frac{T}{L^2/D}. \quad (23)$$

These two results, when substituted into equation (13), give an objective function \mathcal{F} , whose qualitative features are similar to the case of no delay (figure 5(b)). This behavior is what we might anticipate, since delay may be viewed as an additional form of cost.

The primary difference, compared to the no-delay case, is that the optimal Péclet number and the corresponding optimal objective function \mathcal{F} both decrease as the delay time is increased (figure 5). Indeed, delay reduces the number of resetting events/breakdowns, but also induces the coordinate to remain closer to the origin. In the limit where the delay is extremely long, the optimal Péclet number will be small. Moreover, this optimal value will be nearly independent of the cost per breakdown, as the particle will almost never hit the resetting boundary.

3.3. Two dimensions

It is natural to extend the optimization problem of the interval to higher-dimensional domains. Here, we treat the case where the domain is an annulus of outer radius L , inner radius $a < L$, and the diffusing particle is reset to $r = a$ whenever the outer domain boundary is reached. By analogy with the one-dimensional problem, the particle also experiences a drift velocity $v(r) = v_0/r$. As we shall see, the choice of a potential flow field is convenient because the velocity can be combined with the centrifugal term in the Laplacian, which simplifies the form of the solution. A finite inner radius is needed to eliminate the infinite-velocity singularity that would occur if the inner radius was zero.

By close analogy with the finite-interval system, equation (14a), the equation of motion for the particle is

$$\partial_t c + \frac{v}{r} \partial_r c = D \left(\partial_{rr} c + \frac{1}{r} \partial_r c \right) + \delta_a(r) [2\pi r (-D \partial_r c + vc)]|_{r=L}. \quad (24)$$

Here, the flux term has a factor $2\pi r$ due to an integration over all angles. In this geometry, the probability density of finding a particle at a radius r is $2\pi r c(r, t)$. We now introduce the dimensionless variables $x = r/L$, $x_0 = a/L$, the Fourier number $\text{Fo} = Dt/L^2$, and $\text{Pe} = v_0/D$ ⁷ to transform equation (24) into

$$\partial_{\text{Fo}} c(x, \text{Fo}) = \partial_{xx} c(x, \text{Fo}) + \frac{1 - \text{Pe}}{x} \partial_x c(x, \text{Fo}) + \delta_{x_0}(x) [2\pi x (-\partial_x c + \text{Pe} c)]|_{x=1}, \quad (25)$$

and the appropriate boundary conditions for this equation are

$$\begin{cases} [\text{Pe} c(x, \text{Fo}) - x \partial_x c(x, \text{Fo})]|_{x=x_0} = \delta(\text{Fo})/(2\pi) \\ c(1, \text{Fo}) = 0 \\ c(x, 0) = 0. \end{cases}$$

⁷ Note that v_0 is measured in units of velocity times length, so this definition of the Péclet number is dimensionally correct.

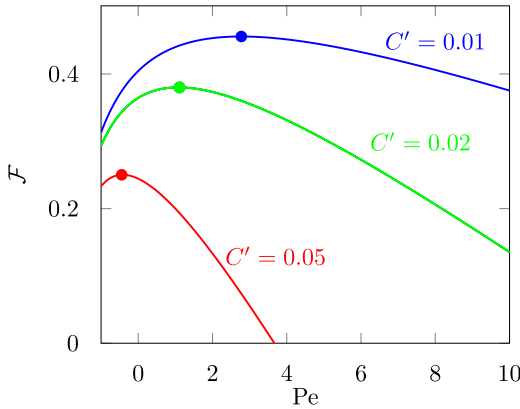


Figure 6. The objective function versus the Péclet number Pe for different normalized cost values $C' \equiv C/(L^2/D)$ in two dimensions.

By performing similar calculations to those performed for the one-dimensional case, we find the following expression for the steady-state probability density in the time domain (see appendix C for details):

$$2\pi x c(x) \simeq \frac{2(\text{Pe} + 2)x(x^{\text{Pe}} - 1)}{\text{Pe}(x_0^2 - 1) - 2x_0^2(x_0^{\text{Pe}} - 1)}. \quad (26)$$

From this expression, the average radial displacement is

$$\langle x \rangle = \int_{x_0}^1 x 2\pi x c(x) dx = \frac{2(\text{Pe} + 2) [\text{Pe}(x_0^3 - 1) - 3x_0^3(x_0^{\text{Pe}} - 1)]}{3(\text{Pe} + 3) [\text{Pe}(x_0^2 - 1) - 2x_0^2(x_0^{\text{Pe}} - 1)]}. \quad (27)$$

The average number of reset events \mathcal{N} satisfies a renewal equation and using \tilde{F}_1 from equation (C.5) we find

$$\tilde{\mathcal{N}}(s) = \frac{1}{s} \frac{1}{\mathcal{W} - 1}, \quad (28a)$$

where

$$\mathcal{W} = x_0^{1+\text{Pe}/2} \sqrt{s} [K_{\text{Pe}/2}(\sqrt{s}) I_{1+\text{Pe}/2}(\sqrt{s}x_0) + I_{\text{Pe}/2}(\sqrt{s}) K_{1+\text{Pe}/2}(\sqrt{s}x_0)],$$

and $I_\nu(x)$ and $K_\nu(x)$ are modified Bessel functions of the first and second kind, respectively. We now extract the long-term behavior for the average number of times that $x = L$ is reached by taking the limit $s \rightarrow 0$ of $\tilde{\mathcal{N}}(s)$. We find

$$\mathcal{N}(t) \simeq \frac{2\text{Pe}(\text{Pe} + 2)}{\text{Pe} + 2x_0^2(x_0^{\text{Pe}} - 1) - \text{Pe} x_0^2} \text{Fo}. \quad (28b)$$

From equations (27) and (28b), we immediately obtain the objective function; representative results are given in figure 6. Overall, the two-dimensional system has the same qualitative behavior as that of one dimension. In the limit $x_0 \rightarrow 0$, the average particle

position $\langle x \rangle$ and the average number of resetting events \mathcal{N} take an even simpler form than that for one dimension:

$$\langle x \rangle \simeq \frac{2(\text{Pe} + 2)}{3(\text{Pe} + 3)} \Theta(\text{Pe} + 2), \quad (29)$$

$$\mathcal{N}(T) \simeq 2(2 + \text{Pe}) \Theta(\text{Pe} + 2) \text{Fo}, \quad (30)$$

where $\Theta(x)$ is the Heaviside step function. The step function arises because of the curious feature that when $\text{Pe} < -2$, the flow field Pe/r at the origin is so strong that the particle remains trapped there forever.

4. Domain growth by first-passage resetting

We now turn to a different aspect of first-passage resetting—the growth of a domain as a result of a diffusing particle that reaches the resetting boundary and causes the boundary to recede by a specified amount at each resetting event. Moving boundaries typically arise at the interface between two thermodynamic phases that undergo a first-order phase transition [43, 44]. In this case, the interface moves continuously as the stable phase grows into the unstable phase. A simple example is water freezing at the interface between water and air, when the air temperature is held below 0°C. A layer of ice grows on top of the water as heat is transported away from the ice-water interface. In this type of system, the temperature field evolves by diffusion and the movement of the interface is determined by the heat flow at the interface.

In contrast, for a growth process that is induced by first-passage resetting, a single diffusing particle is discontinuously reset to a distant location when the boundary is reached. Concomitantly, the motion of the interface is intermittent and discontinuous when the interface recedes by a finite distance upon being reached. A related behavior also occurs in the absence of resetting: returning to the situation depicted in figure 2(a), a boundary that is initially at L moves to $2L$ when it is hit, and then to $3L$, etc. This interface position clearly moves discontinuously, following $\sqrt{4Dt/\pi}$.

In the next paragraphs, we study interface motion and its related properties in the presence of first-passage resetting, when the domain of interest is either a semi-infinite line or a finite interval. We find a variety of growth laws that depend on how far the boundary recedes at each resetting event.

4.1. Expanding semi-infinite geometry

Suppose that the diffusing particle starts at the origin and diffuses in the range $[-\infty, L_n]$, with $L_n > 0$. Each time the particle reaches L_n , the particle is reset to the origin and the interface moves forward by a specified amount δL_n so that $L_{n+1} = L_n + \delta L_n$. Since the resetting events occur at separated discrete times, it is convenient to index the position of the interface by n , the number of resetting events. We consider two natural cases: additive and multiplicative interface growth.

4.1.1. Additive growth: $L_n = L_{n-1} + L$. In this case, the right boundary starts at L and then moves to $2L$ at the first reset event, then to $3L$, etc. We make use of the simple relation between diffusion with resetting and free diffusion, as shown in figure 2. By this equivalence, the probability for n reset events to occur in the time range $[0, t]$ equals the probability that free diffusion travels further than $L_n = n(n+1)L/2$ but no further than $L_{n+1} = (n+1)(n+2)L/2$ in $[0, t]$; that is, the maximum of the freely diffusing particle is located in the range $[L_n, L_{n+1}]$. So, rewriting $\mathcal{M}(t)$ for the average of the maximum $M(t)$, one has

$$\sum_{n \geq 0} L_n P(N(t) = n) \leq \sum_{n \geq 0} \int_{L_n}^{L_{n+1}} dm m P(M(t) = m) \leq \sum_{n \geq 0} L_{n+1} P(N(t) = n),$$

that is

$$\sum_{n \geq 0} L_n P(N(t) = n) \leq \mathcal{M}(t) \leq \sum_{n \geq 0} L_{n+1} P(N(t) = n). \quad (31)$$

This leads to

$$\frac{L}{2} [\langle N^2 \rangle + \langle N \rangle] \leq \mathcal{M}(t) \leq \frac{L}{2} [\langle N^2 \rangle + 3 \langle N \rangle + 2], \quad (32)$$

where we write N for $N(t)$ to simplify the notation, from which it follows that

$$\langle N^2 \rangle \simeq 4 \sqrt{\frac{Dt}{\pi L^2}} \quad \text{or} \quad \sqrt{\langle N^2 \rangle} \simeq 2 \left[\frac{Dt}{\pi L^2} \right]^{\frac{1}{4}}. \quad (33)$$

Note that we do not directly obtain the average number of reset events $\mathcal{N}(t) \equiv \langle N \rangle$ from (33), but only that it scales as $t^{1/4}$. However, we can derive $\mathcal{N}(t)$ by exploiting the renewal structure of the problem in the Laplacian domain (see appendix D) and find

$$\mathcal{N}(t) \simeq \sqrt{\frac{\pi}{2}} \frac{1}{\Gamma(5/4)} \times \left(\frac{t}{\tau} \right)^{1/4}, \quad (34)$$

where $\tau = L^2/D$ is the diffusion time.

The $t^{1/4}$ scaling can be compared with the $t^{1/2}$ scaling that occurs when the boundary is moving through first-passage dynamics but without resetting. When resetting occurs, the number of encounters with the boundary is reduced because after each reset, the boundary is further away. As one might expect, this boundary recession leads to anomalously slow interface growth.

4.1.2. Multiplicative growth: $L_n = \alpha L_{n-1}$, $\alpha > 1$. The approach given above can be applied to multiplicative interface recession. That is, upon the first resetting, the initial boundary at $x = L$ moves to $x = \alpha L$. At the next resetting, the boundary moves from

$x = \alpha L$ to $x = \alpha^2 L$, etc. For this recession rule, equation (31) remains valid, with $L_n = \alpha^n L$. Thus, we have

$$\sum_{n \geq 0} \alpha^n L P(N(t) = n) \leq \mathcal{M}(t) \leq \sum_{n \geq 0} \alpha^{n+1} L P(N(t) = n), \quad (35)$$

from which

$$\langle \alpha^N \rangle L \leq \mathcal{M}(t) \leq \langle \alpha^{N+1} \rangle L. \quad (36)$$

These inequalities suggest that $\mathcal{N}(t)$ scales as $\ln(t/\tau)/2 \ln \alpha$. From the exact Laplace transform approach (see appendix D), we also find the same prefactor in the scaling of $\mathcal{N}(t)$ with t . Thus, we conclude that

$$\mathcal{N}(t) \simeq \ln(t/\tau)/2 \ln \alpha. \quad (37)$$

After n resets, the boundary is located at $\alpha^n L$. We also checked numerically that the distribution of $N(t)$ is concentrated sufficiently tightly around its average value $\mathcal{N}(t)$, so that $\langle \alpha^N \rangle \sim \alpha^{\langle N \rangle} = \alpha^{\mathcal{N}}$. As a result, the average position of the boundary at time t scales according to

$$\alpha^{\mathcal{N}(t)} L \simeq \sqrt{t/\tau} L. \quad (38)$$

Therefore, the boundary moves according to $t^{1/2}$, which is faster than in the additive case, where the boundary moved according to $t^{1/4}$. Despite the smaller number of reset events, each of these events moves the boundary far enough for the overall motion to be almost as fast as in the case of first-passage growth without resetting, with the difference only being a factor of two.

4.2. Expanding interval

We now study the case where a diffusing particle is confined to a finite and growing interval $[0, L_n]$, with a reflecting boundary condition at $x = 0$. Each time the particle reaches the right boundary at $x = L_n$, the particle is instantaneously reset to $x = 0$, while the position of the boundary recedes by a specified amount. We want to understand how the interval grows with time and related statistical properties of this process. We first give the formal result for an arbitrary dependence of L_n on n and then specialize this result to the additive case where $L_n = nL$.

Again, we start with the analog of equation (D.1b) for the finite domain, namely, the Laplace transform of the probability that a reset occurs for the n th time at t :

$$\tilde{R}_n(s) = \tilde{R}_{n-1}(s) \operatorname{sech} \left(\sqrt{s/D} L_n \right) = \prod_{m=1}^n \operatorname{sech} \left(\sqrt{s/D} L_m \right). \quad (39)$$

Here $\operatorname{sech} \left(\sqrt{s/D} L_n \right)$ is the Laplace transform of the first-passage probability to the right boundary of the finite interval $[0, L_n]$ [25]. Similarly, the average number of resetting

events obeys the renewal equation

$$\mathcal{N}(t) = 0 \times Q(L, t) + \sum_{n=1}^{\infty} n \int_0^t dt' Q(L_{n+1}, t - t') R_n(t'), \quad (40a)$$

where $Q(L, t)$ is now the survival probability of a diffusing particle in the finite interval $[0, L_n]$, with reflection at $x = 0$ and absorption at $x = L_n$. In the Laplace domain, equation (40a) becomes

$$\tilde{\mathcal{N}}(s) = \sum_{n=0}^{\infty} n \tilde{Q}(L_{n+1}, s) \tilde{R}_n(s). \quad (40b)$$

Substituting $\tilde{Q}(L_n, s) = [1 - \tilde{F}(L_n, s)]/s$ and equation (D.1b) into the above equation gives

$$\begin{aligned} \tilde{\mathcal{N}}(s) &= \sum_{n=0}^{\infty} \frac{n}{s} \left[1 - \operatorname{sech} \left(\sqrt{s/D} L_{n+1} \right) \right] \prod_{m=1}^n \operatorname{sech} \left(\sqrt{s/D} L_m \right) \\ &= \sum_{n=0}^{\infty} \frac{n}{s} \left[\tilde{R}_n(s) - \tilde{R}_{n+1}(s) \right] = \frac{1}{s} \sum_{n=1}^{\infty} \tilde{R}_n(s) \\ &= \frac{1}{s} \sum_{n=1}^{\infty} \prod_{m=1}^n \operatorname{sech} \left(\sqrt{s/D} L_m \right) \end{aligned} \quad (41)$$

To extract the asymptotic behavior of $\mathcal{N}(t)$, we now focus on the additive case where $L_n = nL$; that is, the boundary recedes by a fixed distance L after each resetting event. Using the dimensionless coordinate $\ell = \sqrt{sL^2/D}$, equation (41) now gives

$$\begin{aligned} \tilde{\mathcal{N}}(s) &= \frac{1}{s} \sum_{n=1}^{\infty} \prod_{m=1}^n \operatorname{sech} \left(\sqrt{s/D} m L \right) = \frac{1}{s} \sum_{n=1}^{\infty} \prod_{m=1}^n \operatorname{sech}(m \ell) \\ &\approx \frac{1}{s} \sum_{n=1}^{\infty} \exp \left\{ \int_0^n dm \ln [\operatorname{sech}(m \ell)] \right\} \\ &\approx \frac{1}{s} \sum_{n=1}^{\infty} \exp \left\{ -\frac{1}{\ell} \left[-\frac{1}{2} \ell^2 n^2 - \frac{1}{2} \operatorname{Li}_2(-e^{2\ell n}) - \ell n \ln 2 - \frac{\pi^2}{24} \right] \right\} \\ &\approx \frac{1}{s\ell} \int_0^{\infty} du \exp \left\{ -\frac{1}{\ell} \left[-\frac{1}{2} u^2 - \frac{1}{2} \operatorname{Li}_2(-e^{2u}) - u \ln 2 - \frac{\pi^2}{24} \right] \right\}. \end{aligned}$$

where $\operatorname{Li}_2(x)$ is the polylogarithm function of order 2. This integral can now be computed in the small s limit using the saddle-point approximation (see appendix E) and the final result is:

$$\tilde{\mathcal{N}}(s) \approx \frac{1}{s\ell} \int_0^{\infty} du \exp \left(-\frac{u^3}{6} \right) \approx \Gamma \left(\frac{4}{3} \right) \frac{1}{s} \left(\frac{6}{\ell^2} \right)^{1/3} + o \left(\frac{1}{s^{4/3}} \right). \quad (42)$$

The Laplace inversion of the above expression gives the average number of resetting events up to time t in the $t \rightarrow \infty$ limit:

$$\mathcal{N}(t) \simeq \left(\frac{6t}{\tau} \right)^{1/3} + o(t^{1/3}). \quad (43)$$

This result implies that the length of the interval also grows according to $t^{1/3}$. To determine the standard deviation (see below), we also need the next correction of the asymptotic behavior. Numerically, we find that $\mathcal{N} \simeq (6t/\tau)^{1/3} + C_1$ where $C_1 = -0.8$.

The $t^{1/3}$ dependence of $\mathcal{N}(t)$ can be understood in a simple way. The mean time for a particle, which starts at $x = 0$, to reach the boundary at $x = L_n$ is $L_n^2/2D = (nL)^2/2D \equiv n^2\tau/2$ [25]. If the particle is immediately reset to the origin each time the boundary is reached, then the time required for \mathcal{N} reset events is $\sum n^2\tau/2 \simeq \mathcal{N}^3\tau/6$. This gives $\mathcal{N} \simeq (6t/\tau)^{1/3}$.

The second moment of the probability distribution for the number of encounters is:

$$\langle \tilde{N}^2(s) \rangle = \sum_{n=0}^{\infty} \frac{n^2}{s} \left[\tilde{R}_n(s) - \tilde{R}_{n+1}(s) \right] = \sum_{n=1}^{\infty} \frac{2n-1}{s} \tilde{R}_n(s) \quad (44)$$

By following similar steps to those used to compute \mathcal{N} , we obtain the following result for fixed values of n and small values of s :

$$\begin{aligned} \langle \tilde{N}^2(s) \rangle &\approx \frac{1}{s\ell} \int_0^\infty du \left(\frac{2u}{\ell} - 1 \right) \\ &\times \exp \left\{ -\frac{1}{\ell} \left[-\frac{1}{2}u^2 - \frac{1}{2}\text{Li}_2(-e^{2u}) - u \ln 2 - \frac{\pi^2}{24} \right] \right\}. \end{aligned}$$

This integral can now be computed in the small- s limit using the saddle-point approximation:

$$\begin{aligned} \langle \tilde{N}^2(s) \rangle &\approx \frac{1}{s\ell} \int_0^\infty du \left(\frac{2u}{\ell} - 1 \right) \exp \left(-\frac{\ell u^3}{6} \right) \\ &\approx \Gamma\left(\frac{5}{3}\right) \frac{1}{s} \left(\frac{6}{\ell^2} \right)^{2/3} + o\left(\frac{1}{s^{5/3}}\right). \end{aligned} \quad (45)$$

Performing a Laplace inversion of the above expression gives:

$$\langle N^2(t) \rangle \simeq \left(\frac{6t}{\tau} \right)^{2/3} + o(t^{2/3}). \quad (46)$$

Numerically, we find that the next correction is $C_2(6t/\tau)^{1/3}$ with $C_2 \approx -1.47$. Hence, the standard deviation grows as $\sqrt{\langle N^2(t) \rangle - \langle N(t) \rangle^2} \approx \sqrt{C_2 - 2C_1} (6t/\tau)^{1/6}$.

Numerical simulations of this growth process (figure 7) show that the distribution of $N(t)$ is highly localized around its average value and rapidly decreases as one moves away from the maximum. While we do not know how to compute the full distribution

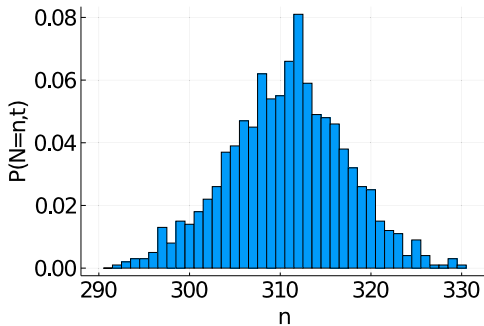


Figure 7. Numerical simulation results for $P(N = n, t)$ for the expanding interval. The initial interval length $L = 1$ and the length grows by one after each resetting event. The distribution is shown at $t = 10^9$ for 1000 walkers. The diffusion constant was set to $\Delta x^2/(2\Delta t) = 5 \times 10^{-3}$.

analytically, we can determine the tails of the distribution by a simple extremal argument [45, 46]. For notational simplicity, we take $L = 1$ and $D = 1$. From the time dependence of the average value of $\mathcal{N}(t)$ (equation (43)), we posit that the natural scaling variable is $z \equiv n/\mathcal{N}(t) \simeq n/t^{1/3}$. We further assume that the distribution can be expressed in the scaling form $P(N = n, t) \propto f(z)$ that decays as a stretched exponential for both $z \rightarrow \infty$ and $z \rightarrow 0$. That is, $f(z) = \exp(-z^a)$, where $a > 0$, for $z \rightarrow \infty$ and $f(z) = \exp(-z^b)$, where $b < 0$, for $z \rightarrow 0$.

Consider now an extreme event in which the particle always moves toward the resetting boundary up until time t . This event occurs with a probability $2^{-t} \sim e^{-t}$. For this directed motion, the particle requires one time step to reach the boundary for the first time, two time steps to reach it for the second time, three time steps for the third time, etc. This leads to a total number, n , of encounters with the boundary that is determined by $\sum_{k=1}^n k = t$. Hence, $n \simeq \sqrt{2t}$. In terms of our scaling function, the probability of reaching the boundary $\sqrt{2t}$ times occurs with a probability of $e^{-t^{a/6}}$. Equating this with e^{-t} gives $a = 6$.

For the small- z tail, we focus on the situation where the boundary is encountered as little as possible. This extremal event is achieved by a random walk that alternately and deterministically moves one step left, then one step right, etc. In this case, the boundary is encountered once and only once. Again, this event occurs with a probability of $2^{-t} \simeq e^{-t}$. On the other hand, this event of a single boundary encounter corresponds to the scaling variable $z = 1/t^{1/3} \rightarrow 0$, and thus occurs with a probability of $e^{-t^{-b/3}}$. Equating these two asymptotic forms of the distribution gives $b = -3$. In summary, we find the following asymptotics:

$$P(N = n, t) \simeq \begin{cases} e^{-(n/\mathcal{N}(t))^6} & n \rightarrow \infty, \\ e^{-(n/\mathcal{N}(t))^{-3}} & n \rightarrow 0. \end{cases} \quad (47)$$

Because the exponent values in the scaling forms are fairly large, it does not seem possible to verify these asymptotic behaviors numerically.

5. Summary and discussion

We presented the concept of first-passage resetting, in which a random walk is reset to its starting point whenever it reaches a specified location. This situation contrasts with constant-rate resetting, in which a random walk is reset to its starting point at a fixed rate. In the case of a semi-infinite line $[-\infty, L]$, with $L > 0$, the particle diffuses freely and is reset to the origin whenever it reaches L . The resulting probability distribution has dramatically different behaviors, depending on whether $0 < x < L$ or $x < 0$. In the former case, the distribution has a simple linear profile that arises from the balance between the flux leaving at the reset point and the flux being reinjected at $x = 0$. In the latter case, the probability distribution reduces to free diffusion in the presence of a reflecting boundary. We derived this result analytically and also via a path decomposition that is reminiscent of the image method.

In the finite-interval geometry, we defined an optimization problem that describes, in a schematic way, aspects of the repeated breakdown of a driven mechanical system. The operational domain of the system is a finite interval; this interval could be interpreted as the RPM range of an engine. The resetting boundary corresponds the system reaching its operating limit or maximum RPMs, after which a breakdown occurs and the system has to be restarted from scratch. The control parameter is the bias velocity (not to be confused with the RPM of the engine), which may either drive the system toward breakdown or toward minimal-level operation. We showed that an optimal bias velocity exists, which optimizes the performance of the system. This optimum balances the gain by operating close to $x = L$ while minimizing the number of breakdowns. A similar physical picture arises if breakdown is accompanied by a random delay before restarting the system or by extension to a two-dimensional geometry.

We also studied a variety of domain-growth phenomena that are driven by first-passage dynamics with resetting. When each resetting event moves the boundary by a fixed amount, the boundary recedes according to $t^{1/4}$ and as $t^{1/3}$ for the semi-infinite geometry and the finite interval, respectively. In the semi-infinite geometry, if the boundary position grows by a factor $\alpha > 1$ with each resetting event, then the interface moves much more quickly, at $t^{1/2}$. The case where the boundary moves by a fixed amount at each resetting is actually a version of the internal diffusion-limited aggregation problem, for which there is extensive literature that has focused on the geometrical properties of growing domains (see, e.g. [47–50]). We instead focused on the rich dynamic aspects of the model and we suggest, based on the correspondence with internal diffusion-limited aggregation, that it will be worthwhile to treat our first-passage resetting in a finite two-dimensional domain.

There are a variety of extensions of the optimization problem that may be worth exploring. First, the control strategy could be finer than a simple uniformly biased velocity [51]. More realistically, one could also associate a cost with a strategy that becomes more expensive as the control mechanism becomes more sophisticated. For instance, it would be natural to turn on a bias velocity *away* from the breakdown point when the system is very close to breakdown. It would also be useful to identify the optimal region over which the particle experiences a bias (both toward and away from the breakdown point). In addition to a more refined control strategy, other simple

geometries may be worth studying. One such example is a one-dimensional interval with a first-passage resetting mechanism at each end of the interval that has a different cost for reaching each end. First-passage resetting in a bounded planar geometry with a cost function that depends on the angle at which the boundary is hit might be another geometry that would be worth studying.

Given the rich behavior exhibited by first-passage resetting, it should also be worthwhile to investigate extensions of the basic model, as well as applications. An example of the former is the Fleming–Viot branching process, in which there are $N + 1$ particles and when one of them resets, it resets to one of the positions of the remaining N particles [52–56]. More generally, first-passage resetting in the presence of multiple diffusing particles could lead to new phenomenology. On another note, applications also exist in cash flow management: cash levels in a large firm are sometimes modeled as a diffusion process in which one wishes to have cash fully invested in profitable ventures, while at the same time keeping enough cash available so as to avoid being indebted [57, 58]. These types of problem seem to be ripe for further exploration.

Acknowledgments

B B’s research at the Perimeter Institute was supported in part by the Government of Canada through the Department of Innovation, Science and Economic Development, Canada and by the Province of Ontario through the Ministry of Colleges and Universities. J R F’s research at Columbia University was supported by the Alliance Program. S R thanks Paul Hines for helpful conversations and financial support from NSF Grant DMR-1910736. We thank one of the referees for providing helpful suggestions about possible extensions of the basic optimization problem.

Appendix A. Laplace transform approach in semi-infinite geometry

A.1. Spatial probability distributions

The probability distribution $P(x, t)$ of a diffusing particle at time t on a semi-infinite line $x \leq L$, can be obtained in several ways. In the main text, we presented a path-transformation approach and here, we detail the Laplace transform approach (see also [34]). We first partition the trajectory according to the number of reset events up to time t . Between consecutive resets, the particle undergoes free diffusion with an absorbing boundary at $x = L$. This part of the motion is described by the free propagator

$$G(x, L, t) = \left[e^{-x^2/4Dt} - e^{-(x-2L)^2/4Dt} \right] / \sqrt{4\pi Dt}, \quad (\text{A.1})$$

which can be computed, for example, by the image method [24, 25]. Summing over all reset events, the spatial probability is determined by

$$P(x, t) = G(x, L, t) + \sum_{n \geq 1} \int_0^t dt' F_n(L, t') G(x, L, t-t'). \quad (\text{A.2a})$$

Equation (A.2a) states that for the particle to be at x at time t , it either: (i) must never hit L , in which case its probability distribution is just $G(x, L, t)$, or (ii), the particle first hits L for the n th time at $t' < t$, after which the particle restarts at the origin and then propagates to x in the remaining time $t - t'$ without hitting L again. The equivalent way of writing equation (A.2a) in a renewal fashion is:

$$P(x, t) = G(x, L, t) + \int_0^t dt' F_1(L, t') P(x, t - t'). \quad (\text{A.2b})$$

The first term accounts for the particle never reaching $x = L$, while the second term accounts for the particle reaching $x = L$ at a time t' , after which the process starts anew from $x(t') = 0$ for the remaining time $t - t'$. Note that this is a renewal equation in the sense that the second term contains the full propagator $P(x, t - t')$ and not the free propagator $G(x, t - t')$, thereby accounting for any number of resetting events in the time interval $[t', t]$.

To solve for $P(x, t)$ we again treat the problem in the Laplace domain. While we can find the solution from the Laplace transform of equation (A.2a), the solution is simpler and more direct from the Laplace transform of (A.2b):

$$\tilde{P}(y, s) = \tilde{G}(y, \ell, s) + \tilde{F}_1(\ell, s) \tilde{P}(y, s), \quad (\text{A.3a})$$

with

$$\tilde{G}(y, \ell, s) = [e^{-|y|} - e^{-|y-2\ell|}] / \sqrt{4Ds}$$

i.e. the Laplace transform of $G(x, L, t)$, where we have introduced the scaled coordinates $y \equiv x\sqrt{s/D}$ and $\ell \equiv L\sqrt{s/D}$. Solving for $\tilde{P}(y, s)$ yields:

$$\tilde{P}(y, s) = \frac{\tilde{G}(y, \ell, s)}{1 - \tilde{F}_1(\ell, s)} = \frac{1}{\sqrt{4Ds}} \frac{[e^{-|y|} - e^{-|y-2\ell|}]}{1 - e^{-\ell}}. \quad (\text{A.3b})$$

To invert this Laplace transform, we separately consider the cases $0 \leq y \leq \ell$ and $y < 0$. In the former, we expand the denominator in a Taylor series to give

$$\begin{aligned} \tilde{P}(y, s) &= \frac{1}{\sqrt{4Ds}} [e^{-y} - e^{-(2\ell-y)}] \sum_{n \geq 0} e^{-n\ell} \\ &= \frac{1}{\sqrt{4Ds}} \sum_{n \geq 0} [e^{-(y+n\ell)} - e^{-[(n+2)\ell-y]}], \quad 0 < y \leq \ell, \end{aligned} \quad (\text{A.4a})$$

from which

$$P(x, t) = \frac{1}{\sqrt{4\pi Dt}} \sum_{n \geq 0} \left[e^{-(x+nL)^2/4Dt} - e^{-[x-(n+2)L]^2/4Dt} \right], \quad 0 < x \leq L. \quad (\text{A.4b})$$

In the case of $y < 0$, $\tilde{P}(y, s)$ in equation (A.3b) is factorizable:

$$\tilde{P}(y, s) = \frac{1}{\sqrt{4Ds}} \left[\frac{e^y - e^{y-2\ell}}{1 - e^{-\ell}} \right] = \frac{1}{\sqrt{4Ds}} [e^y + e^{(y-\ell)}], \quad (\text{A.5a})$$

and this latter form can readily be inverted to give:

$$P(x, t) = \frac{1}{\sqrt{4\pi Dt}} \left[e^{-x^2/4Dt} + e^{-(x-L)^2/4Dt} \right] \quad x < 0. \quad (\text{A.5b})$$

A.2. Average number of resets

The average number of resets that occur up to time t may also be derived using the Laplace transform approach. The probability for n resets to occur by time t equals the probability of having at least n resets, minus the probability of having at least $n+1$ resets:

$$\begin{aligned} P(N(t)=n) &= P(N(t) \geq n) - P(N(t) \geq n+1), \\ &= \int_0^t dt' F_n(L, t') - \int_0^t dt' F_{n+1}(L, t'). \end{aligned} \quad (\text{A.6a})$$

Using our earlier result that $F_n(L, t) = F_1(nL, t)$, we have

$$P(N(t)=n) = \text{erf}\left(\frac{(n+1)L}{\sqrt{4Dt}}\right) - \text{erf}\left(\frac{nL}{\sqrt{4Dt}}\right), \quad (\text{A.6b})$$

where erf is the Gauss error function.

We can compute the average number of reset events, $\mathcal{N}(t) \equiv \langle N(t) \rangle$, from (7), but it is quicker to use a renewal equation approach. Here we can write

$$\mathcal{N}(t) = \int_0^t dt' F_1(L, t-t') [1 + \mathcal{N}(t')]. \quad (\text{A.7a})$$

Equation (A.7a) states that to have \mathcal{N} reset events up to time t , $\mathcal{N}-1$ reset events must have occurred at some earlier time $t' < t$, and then one more reset event occurs exactly at time t . Taking the Laplace transform of (A.7a) gives

$$\tilde{\mathcal{N}}(s) = \frac{\tilde{F}_1(L, s)}{s(1 - \tilde{F}_1(L, s))} = \frac{e^{-\ell}}{s(1 - e^{-\ell})}, \quad (\text{A.7b})$$

where again $\ell = L\sqrt{s/D}$. We extract the long-time behavior of the average number of reset events by taking the $s \rightarrow 0$ limit and then performing Laplace inversion on this limiting expression. We thus find

$$\mathcal{N}(t) \simeq \sqrt{4Dt/\pi L^2}. \quad (\text{A.8})$$

Appendix B. Solution to the convection–diffusion equation

The general solution to equation (14b) is

$$\tilde{c}_0(x, s) = e^P (A e^{wx} + B e^{-wx}), \quad (\text{B.1})$$

where $P = vx/2D$, $w = \sqrt{v^2 + 4Ds}/2D$, and A, B are integration constants. To determine A and B , we apply the boundary conditions that accompany equation (B.1) to give the linear system

$$\begin{cases} v(A + B) - \frac{1}{2}v(A + B) - ADw + BDw = 1, \\ e^{vL/(2D)} (A e^{Lw} + B e^{-Lw}) = 0, \end{cases} \quad (\text{B.2})$$

whose solution is

$$\begin{cases} A = -\frac{2}{2Dw e^{2Lw} + 2Dw + v e^{2Lw} - v} = -\frac{e^{-Lw}}{2Dw \cosh(Lw) + v \sinh(Lw)}, \\ B = \frac{2e^{2Lw}}{2Dw e^{2Lw} + 2Dw + v e^{2Lw} - v} = \frac{e^{Lw}}{2Dw \cosh(Lw) + v \sinh(Lw)}. \end{cases} \quad (\text{B.3})$$

We define $\mathcal{W} \equiv 2Dw \cosh(Lw) + v \sinh(Lw)$, from which $A = -e^{-Lw}/\mathcal{W}$ and $B = e^{Lw}/\mathcal{W}$. Substituting these constants back into the general solution equation (B.1) leads to equation (15a).

Appendix C. First-passage resetting in the annular geometry

For the convection–diffusion equation in two dimensions with a radial drift v/r ; that is, equation (25) without the delta-function term, the general solution in the Laplace domain is [59]

$$\tilde{c}_0(x, s) = x^{\text{Pe}/2} [A I_{\text{Pe}/2}(\sqrt{s}x) + B K_{\text{Pe}/2}(\sqrt{s}x)], \quad (\text{C.1})$$

where A and B are integration constants, and $I_\nu(x)$ and $K_\nu(x)$ are modified Bessel functions of the first and second kind, respectively. The subscript 0 refers to the concentration without flux re-injection. Imposing the boundary conditions that accompany equation (25) leads to a linear system to solve for A and B :

$$\begin{cases} A I_{\text{Pe}/2}(\sqrt{s}) + B K_{\text{Pe}/2}(\sqrt{s}) = 0, \\ \sqrt{s}x_0^{1+\text{Pe}/2} (B K_{1+\text{Pe}/2}(\sqrt{s}x_0) - A I_{1+\text{Pe}/2}(\sqrt{s}x)) = 1/(2\pi). \end{cases} \quad (\text{C.2})$$

whose solution is:

$$\begin{cases} A = -\frac{x_0^{-(1+\text{Pe}/2)} K_{\text{Pe}/2}(\sqrt{s})}{2\pi\sqrt{s} (K_{\text{Pe}/2}(\sqrt{s}) I_{1+\text{Pe}/2}(\sqrt{s}x_0) + I_{\text{Pe}/2}(\sqrt{s}) K_{1+\text{Pe}/2}(\sqrt{s}x_0))}, \\ B = \frac{x_0^{-(1+\text{Pe}/2)} I_{\text{Pe}/2}(\sqrt{s})}{2\pi\sqrt{s} (K_{\text{Pe}/2}(\sqrt{s}) I_{1+\text{Pe}/2}(\sqrt{s}x_0) + I_{\text{Pe}/2}(\sqrt{s}) K_{1+\text{Pe}/2}(\sqrt{s}x_0))}. \end{cases} \quad (\text{C.3})$$

We now define $\mathcal{W} \equiv x_0^{1+\text{Pe}/2} \sqrt{s} [K_{\text{Pe}/2}(\sqrt{s}) I_{1+\text{Pe}/2}(\sqrt{s}x_0) + I_{\text{Pe}/2}(\sqrt{s}) K_{1+\text{Pe}/2}(\sqrt{s}x_0)]$. In terms of this function, we have $A = K_{\text{Pe}/2}(\sqrt{s}) / (2\pi\mathcal{W})$ and $B = I_{\text{Pe}/2}(\sqrt{s}) / (2\pi\mathcal{W})$. Substituting these constants back into equation (C.1) yields:

$$\tilde{c}_0(x, s) = \frac{x^{\text{Pe}/2} [I_{\text{Pe}/2}(\sqrt{s}) K_{\text{Pe}/2}(\sqrt{s}x) - K_{\text{Pe}/2}(\sqrt{s}) I_{\text{Pe}/2}(\sqrt{s}x)]}{2\pi\mathcal{W}}, \quad (\text{C.4})$$

The first-passage probability is obtained by computing the outlet flux at $x = 1$ from the concentration in equation (C.4):

$$\begin{aligned} \tilde{F}_1(s) &= 2\pi (-x\partial_x \tilde{c}_0(x, s) + \text{Pe} \tilde{c}_0(x, s))|_{x=1} \\ &= 2\pi (-\partial_x \tilde{c}_0(x, s))|_{x=1} \\ &= \frac{\sqrt{s} I_{\text{Pe}/2}(\sqrt{s}) K_{1-\text{Pe}/2}(\sqrt{s}) + \sqrt{s} I_{1-\text{Pe}/2}(\sqrt{s}) K_{\text{Pe}/2}(\sqrt{s})}{\mathcal{W}} = \frac{1}{\mathcal{W}}, \end{aligned} \quad (\text{C.5})$$

where we used the absorbing boundary condition to obtain the second line.

On the other hand, the survival probability, $Q(t)$, is defined as the integral of $2\pi x \tilde{c}_0(x, t)$ over the interval $[x_0, 1]$. Alternatively, it can be computed as the probability of not having hit the absorbing boundary before time t : $Q(t) = 1 - \int_0^t dt' F_1(t')$, which in the Laplace domain translates to $\tilde{Q}(s) = (1 - \tilde{F}_1(s))/s$. Using equation (C.5), we obtain:

$$\tilde{Q}(s) = \frac{1}{s} \left(1 - \frac{1}{\mathcal{W}}\right). \quad (\text{C.6})$$

When there is re-injection of the outgoing flux, the concentration obeys the renewal equation below. In the Laplace domain and using the form for \tilde{c}_0 obtained above, we find:

$$\tilde{c}(x, s) = \frac{\tilde{c}_0(x, s)}{1 - \tilde{F}_1(s)} = \frac{x^{\text{Pe}/2} [I_{\text{Pe}/2}(\sqrt{s}) K_{\text{Pe}/2}(\sqrt{s}x) - K_{\text{Pe}/2}(\sqrt{s}) I_{\text{Pe}/2}(\sqrt{s}x)]}{2\pi(\mathcal{W} - 1)}. \quad (\text{C.7})$$

In the $s \rightarrow 0$ limit, we find that:

$$\begin{aligned} x^{\text{Pe}/2} [I_{\text{Pe}/2}(\sqrt{s}) K_{\text{Pe}/2}(\sqrt{s}x) - K_{\text{Pe}/2}(\sqrt{s}) I_{\text{Pe}/2}(\sqrt{s}x)] &\simeq \frac{1 - x^{\text{Pe}}}{\text{Pe}}, \\ \mathcal{W} - 1 &\simeq \frac{\text{Pe} - \text{Pe} x_0^2 + 2x_0^2 (-1 + x_0^{\text{Pe}})}{2\text{Pe}(2 + \text{Pe})} s. \end{aligned} \quad (\text{C.8})$$

Substituting these asymptotic expressions into equation (C.7), the coefficient of the term proportional to $1/s$ in $\tilde{c}(x, s)$ gives the steady-state probability density in the time domain that is quoted in equation (26).

Appendix D. Expanding semi-infinite geometry: Laplace transforms

Here, using Laplace transforms, we derive the properties for domain growth in the semi-infinite geometry that were obtained in the main text using a path transformation. Suppose that the diffusing particle starts at the origin and diffuses in the range $[-\infty, L_n]$, with $L_n > 0$. Each time the particle reaches L_n , the particle is reset to the origin and the interface moves forward by a specified amount δL_n so that $L_{n+1} = L_n + \delta L_n$. Since the resetting events occur at separate discrete times, it is convenient to index the position of the interface by n , the number of resetting events. We consider two natural cases: additive and multiplicative interface growth.

D.1. Additive growth: $L_n = L_{n-1} + L$

In this case, the right boundary starts at L and then moves to $2L$ at the first reset event, then to $3L$, etc. The probability that the n th reset occurs at time t , $R_n(t)$, is given by the renewal equation

$$R_n(t) = \int_0^t dt' R_{n-1}(t-t') F(L_n=nL, t'), \quad (\text{D.1a})$$

where $F(L_1, t)$ is the standard first-passage probability of reaching L_1 when the particle starts from the origin. In the Laplacian domain, equation (D.1a) becomes

$$\tilde{R}_n(s) = \tilde{R}_{n-1}(s) e^{-n\ell} = e^{-n(n+1)\ell/2}, \quad (\text{D.1b})$$

with $\ell \equiv \sqrt{sL^2/D}$.

By a similar consideration, the average number of resetting events is

$$\mathcal{N}(t) = 0 \times Q(L, T) + \sum_{n=1}^{\infty} n \int_0^t dt' Q((n+1)L, t-t') R_n(t'), \quad (\text{D.2a})$$

which, in the Laplace domain, becomes

$$\tilde{\mathcal{N}}(s) = \sum_{n=0}^{\infty} n \tilde{Q}((n+1)L, s) \tilde{R}_n(s). \quad (\text{D.2b})$$

Here $Q(L, t) = 1 - \int_0^T dt F(L, t)$ is the survival probability for a diffusing particle that starts at the origin to fail to reach an absorbing boundary at L within time T .

In the Laplace domain, this relation becomes $\tilde{Q}(nL, s) = [1 - \tilde{F}(nL, s)]/s$. We now substitute this expression for \tilde{Q} and the above expression for $\tilde{R}_n(s)$ into (D.2b), and

then convert the sum to an integral to give

$$\begin{aligned}\tilde{\mathcal{N}}(s) &\approx \int_0^\infty dn \frac{n}{s} [1 - e^{-(n+1)\ell}] e^{-n(n+1)\ell/2} \\ &= \frac{e^{-\ell}}{4s\ell} \left\{ \sqrt{2\pi\ell} e^{9\ell/8} \left[2 + \operatorname{erf}(\sqrt{\ell/8}) - 3\operatorname{erf}(3\sqrt{\ell/8}) \right] + 4e^\ell - 4 \right\} \\ &\rightarrow \frac{1}{s} \sqrt{\frac{\pi}{2\ell}} \quad s \rightarrow 0.\end{aligned}\tag{D.3a}$$

Taking the Laplace inverse of this expression, the average number of reset events asymptotically scales as

$$\mathcal{N}(t) \simeq \sqrt{\frac{\pi}{2}} \frac{1}{\Gamma(5/4)} \times \left(\frac{t}{\tau} \right)^{1/4},\tag{D.3b}$$

where $\tau = L^2/D$ is the diffusion time.

D.2. Multiplicative growth: $L_n = \alpha L_{n-1}$, $\alpha > 1$

The approach given above can be applied to multiplicative interface recession. That is, upon the first resetting, the initial boundary at $x = L$ moves to $x = \alpha L$. In the next resetting, the boundary moves from $x = \alpha L$ to $x = \alpha^2 L$, etc. For this recession rule, the probability of the n th reset event occurring at time at t , $R_n(t)$, is

$$R_n(t) = \int_0^t dt' R_{n-1}(t-t') F(\alpha^{n-1}L, t'),\tag{D.4a}$$

which, in the Laplace domain, becomes

$$\tilde{R}_n(s) = \tilde{R}_{n-1}(s) e^{-\sqrt{s/D} \alpha^{n-1} L} \equiv \tilde{R}_{n-1}(s) e^{-\ell \alpha^{n-1}} = e^{-\ell (1-\alpha^n)/(1-\alpha)}.\tag{D.4b}$$

The average number of reset events before time t is

$$\mathcal{N}(t) = 0 \times Q(L, T) + \sum_{n=1}^{\infty} n \int_0^t dt' Q(\alpha^n L, t-t') R_n(t'),\tag{D.5a}$$

which becomes, in the Laplace domain,

$$\tilde{\mathcal{N}}(s) = \sum_{n=0}^{\infty} n \tilde{Q}(\alpha^n L, s) \tilde{R}_n(s).\tag{D.5b}$$

Substituting $\tilde{Q}(\alpha^n L, s) = [1 - \tilde{F}(\alpha^n L, s)]/s$ and (D.4b) into the above equation, we obtain

$$\begin{aligned}
\tilde{\mathcal{N}}(s) &= \sum_{n=0}^{\infty} \frac{n}{s} (1 - e^{-\ell\alpha^n}) e^{-\ell(1-\alpha^n)/(1-\alpha)} \\
&\approx \int_0^{\infty} dn \frac{n}{s} (1 - e^{-\ell\alpha^n}) e^{-\ell(1-\alpha^n)/(1-\alpha)} \\
&= \frac{1}{s} e^{-\ell/(1-\alpha)} \int_0^{\infty} dn n (1 - e^{-\ell\alpha^n}) e^{\ell\alpha^n/(1-\alpha)}. \tag{D.6}
\end{aligned}$$

To evaluate the above integral, we make the variable change $z = u\alpha^{n-1}$, from which $n = \ln(z\alpha/u)/\ln\alpha$ and $dn = dz/(z\ln\alpha)$. The above integral now becomes:

$$\tilde{\mathcal{N}}(s) = \frac{1}{s} \frac{e^{-\ell/(1-\alpha)}}{(\ln\alpha)^2} \int_{\ell/\alpha}^{\infty} dz \frac{\ln(z\alpha/u)}{z} (1 - e^{-\alpha z}) e^{\alpha z/(1-\alpha)},$$

For $s \rightarrow 0$, we compute the above integral by first splitting it into two terms, using $\ln(z\alpha/u) = \ln z + \ln(\alpha/u)$. The contribution from the first term is finite, while the second one diverges. Dropping the finite term, we obtain

$$\tilde{\mathcal{N}}(s) \simeq \frac{\ln(\alpha/u)}{s} \frac{e^{-\ell/(1-\alpha)}}{(\ln\alpha)^2} \int_{\ell/\alpha}^{\infty} dz \frac{1 - e^{-\alpha z}}{z} e^{\alpha z/(1-\alpha)} \simeq -\frac{\ln(s\tau)}{2s \ln\alpha}, \quad s \rightarrow 0. \tag{D.7}$$

Note that we introduce the factor τ inside the logarithm, so that this term is manifestly dimensionless. Thus, in the long-term limit, the average number of resetting events scales as

$$\mathcal{N}(t) \simeq \frac{\ln(t/\tau)}{2 \ln\alpha}. \tag{D.8}$$

Appendix E. Expanding interval: saddle point approximation

We want to compute the following integral in the small ℓ limit:

$$I(\ell) = \int_0^{\infty} du \exp \left[-\frac{1}{\ell} f(u) \right], \tag{E.1}$$

where $f(u) = -\frac{1}{2}u^2 - \frac{1}{2}\text{Li}_2(-e^{2u}) - u \log(2) - \frac{\pi^2}{24}$. Because the negative exponential rapidly decreases as $\ell \rightarrow 0$, the main contribution will occur when $f(u)$ is at a minimum. This function has a global minimum located at $u = 0$ and can be locally approximated by $f(u) \simeq u^3/6$. Substituting this into equation (E.1), we recover equation (42).

References

- [1] Chandrasekhar S 1943 *Rev. Mod. Phys.* **15** 1
- [2] Van Kampen N G 1992 *Stochastic Processes in Physics and Chemistry* vol 1 (Amsterdam: Elsevier)
- [3] Chicheportiche R and Bouchaud J P 2014 Some applications of first-passage ideas to finance *First-passage Phenomena and Their Applications* (Singapore: World Scientific) pp 447–76

- [4] Rogers E M 2010 *Diffusion of Innovations* (Simon and Schuster)
- [5] Weiss G H 1994 *Aspects and Applications of the Random Walk* (Amsterdam: North-Holland)
- [6] Hughes B D *et al* 1995 *Random Walks and Random Environments: Random Walks* vol 1 (Oxford: Oxford University Press)
- [7] Rudnick J and Gaspari G 2004 *Elements of the Random Walk: An Introduction for Advanced Students and Researchers* (Cambridge: Cambridge University Press)
- [8] Klafter J and Sokolov I M 2011 *First Steps in Random Walks: From Tools to Applications* (Oxford: Oxford University Press)
- [9] Evans M R and Majumdar S N 2011 *Phys. Rev. Lett.* **106** 160601
- [10] Evans M R and Majumdar S N 2011 *J. Phys. A: Math. Theor.* **44** 435001
- [11] Evans M R, Majumdar S N and Schehr G 2020 *J. Phys. A: Math. Theor.* **53** 193001
- [12] Boyer D and Solis-Salas C 2014 *Phys. Rev. Lett.* **112** 240601
- [13] Christou C and Schadschneider A 2015 *J. Phys. A: Math. Theor.* **48** 285003
- [14] Rotbart T, Reuveni S and Urbakh M 2015 *Phys. Rev. E* **92** 060101
- [15] Majumdar S N, Sabhapandit S and Schehr G 2015 *Phys. Rev. E* **92** 052126
- [16] Reuveni S 2016 *Phys. Rev. Lett.* **116** 170601
- [17] Pal A and Reuveni S 2017 *Phys. Rev. Lett.* **118** 030603
- [18] Belan S 2018 *Phys. Rev. Lett.* **120** 080601
- [19] Bodrova A S, Chechkin A V and Sokolov I M 2019 *Phys. Rev. E* **100** 012119
- [20] Kuśmierz L and Gudowska-Nowak E 2015 *Phys. Rev. E* **92** 052127
- [21] Campos D and Méndez V 2015 *Phys. Rev. E* **92** 062115
- [22] Bhat U, De Bacco C and Redner S 2016 *J. Stat. Mech.* **083401**
- [23] Eule S and Metzger J J 2016 *New J. Phys.* **18** 033006
- [24] Feller W 2008 *An Introduction to Probability Theory and its Applications* vol 1 (New York: Wiley)
- [25] Redner S 2001 *A Guide to First-Passage Processes* (Cambridge: Cambridge University Press)
- [26] Bray A J, Majumdar S N and Schehr G 2015 *Adv. Phys.* **62** 225–361
- [27] Feller W 1954 *Trans. Am. Math. Soc.* **77** 1
- [28] Sherman B 1958 *Ann. Math. Stat.* **29** 267–73
- [29] Falcao R and Evans M R 2017 *J. Stat. Mech.* **023204**
- [30] Ross S M 2014 *Introduction to Probability Models* (New York: Academic)
- [31] Gnedenko B V, Belyayev Y K and Solov'yev A D 2014 *Mathematical Methods of Reliability Theory* (New York: Academic)
- [32] Ajjarapu V, Lau P L and Battula S 1994 *IEEE Trans. Power Syst.* **9** 906–17
- [33] Feng Z, Ajjarapu V and Maratukulam D J 2000 *IEEE Trans. Power Syst.* **15** 791–7
- [34] De Bruyne B, Randon-Furling J and Redner S 2020 *Phys. Rev. Lett.* **125** 050602
- [35] Lévy P 1948 *Processus stochastiques et mouvement brownien* (Paris: Gauthier-Villars)
- [36] Borodin A N and Salminen P 2012 *Handbook of Brownian Motion—Facts and Formulae* (Basel: Birkhäuser)
- [37] Bachelier L 1900 *Ann. Sci. École Norm. Sup.* **17** 21–86
- [38] Lévy P 1940 *Compos. Math.* **7** 283–339
- [39] Krapivsky P L and Redner S 2018 *J. Stat. Mech.* **093208**
- [40] Gallavotti G and McKean H P 1972 *Nagoya Math. J.* **47** 1–14
- [41] Harrison J M and Lemoine A J 1981 *J. Appl. Probab.* **18** 216–26
- [42] Bou-Rabee N and Holmes-Cerfon M C 2020 *SIAM Rev.* **62** 164–95
- [43] Crank J 1987 *Free and Moving Boundary Problems* (Oxford: Oxford University Press)
- [44] Rubinstein L 2000 *The Stefan Problem* vol 8 (Providence, RI: American Mathematical Society)
- [45] Fisher M E 1966 *J. Chem. Phys.* **44** 616–22
- [46] Krapivsky P L, Redner S and Ben-Naim E 2010 *A Kinetic View of Statistical Physics* (Cambridge: Cambridge University Press)
- [47] Meakin P and Deutch J M 1986 *J. Chem. Phys.* **85** 2320–5
- [48] Lawler G F, Bramson M and Griffeath D 1992 *Ann. Probab.* **20** 2117–40
- [49] Moore C and Machta J 2000 *J. Stat. Phys.* **99** 661–90
- [50] Jerison D, Levine L and Sheffield S 2012 *J. Am. Math. Soc.* **25** 271–301
- [51] Lunz D 2020 *J. Phys. A: Math. Theor.* **53** 44LT01
- [52] Fleming W and Viot M 1979 *Indiana Univ. Math. J.* **28** 817–43
- [53] Burdzy K, Holyst R, Ingerman D and March P 1996 *J. Phys. A: Math. Gen.* **29** 2633
- [54] Burdzy K, Holyst R and March P 2000 *Commun. Math. Phys.* **214** 679–703
- [55] Grigorescu I and Kang M 2004 *Stoch. Process. Appl.* **110** 111–43

Optimization and growth in first-passage resetting

- [56] Grigorescu I *et al* 2006 *Electron. J. Probab.* **11** 311–31
- [57] Harrison J M, Sellke T M and Taylor A J 1983 *Math. Oper. Res.* **8** 454–66
- [58] Buckholtz P G, Campbell L L, Milbourne R D and Wasan M T 1983 *J. Appl. Probab.* **20** 61–70
- [59] Abramowitz M, Stegun I A and Romer R H 1965 *Handbook of Mathematical Functions with Formulas, Graphs, and Mathematical Tables* (Washington, DC: Dover)